Submitted to: HALO '03 and Beam-Beam Workshop
Montauk, NY, June 19-23, 2003

BNL-71291-2003-CP

Longitudinal Mismatch in SCL as a Source of Beam Halo*

Alessandro G. Ruggiero
(E-mail: agr@bnl.gov)
Brookhaven National Laboratory, Upton, NY 11973

Abstract. An advantage of a proton Super-Conducting Linac (SCL) is that RF cavities can be operated independently, allowing easier beam transport and acceleration. But cavities are to be separated by drifts long enough to avoid they couple to each other. Moreover, cavities are placed in cryostats that include inactive insertions for cold-warm transitions; and interspersed are warm insertions for magnets and other devices. The SCL is then an alternating sequence of accelerating elements and drifts. No periodicity is present, and the longitudinal motion is not adiabatic. This has the consequence that the beam bunch ellipse will tumble, dilute and create a halo in the momentum plane because of inherent nonlinearities. When this is coupled to longitudinal space-charge forces, it may cause beam loss with latent activation of the accelerator components.

THE AGS SUPERCONDUCTING LINAC

At BNL we have few projects that require Super-Conducting Linacs (SCL). One of them is the AGS Upgrade for a proton average power of 1 MWatt (Ref. 1). The location of the AGS-SCL is shown in Figure 1. It follows the 200-MeV Room Temperature Linac and accelerates negative ions to 1.2 GeV for multi-turn, charge-exchange injection into the AGS.

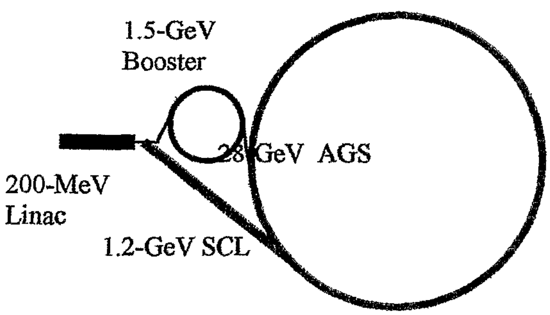

Figure 1. The AGS complex with the 1.2-GeV SCL

The SCL is made of three sections, as shown in Figure 2, that are: the Low-Energy (LE) section from 200 to 400 MeV, the Medium-Energy (ME) section from 400 to 800 MeV, and the High-Energy (HE) section to the final 1.2 GeV. The first section operates at 805 MHz, the last two at 1,610 MHz.

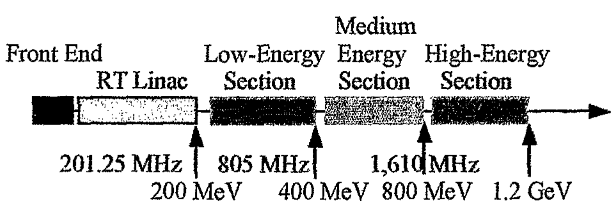

Figure 2. Layout of the AGS-SCL with three Sections

* Work performed under the auspices of the U.S. Department of Energy

Any of the three sections is made of a sequence of identical Periods, each made of a Warm Insertion for quadrupoles and other beam devices, and a Cryomodule inside which cavities are located, as shown in Figure 3. Each Cryomodule is made of M Cavities, and each cavity is made of N cells. Cavities are separated from each other by a distance d large enough for the insertion of RF couplers and for decoupling. Each end of a Cryomodule has in addition a transition from the cold to the warm region that takes space. Finally Cryomodules are separated by the Warm Insertions that take an extensive length.

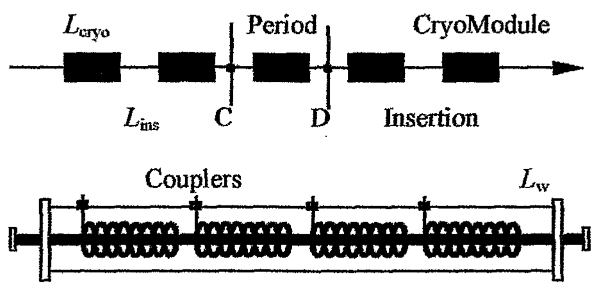

Figure 3. Sequence of Periods, Cavities, Cells and Warm Insertions in one SCL Section

Thus a section of SCL is made of a alternating sequence of Drifts of different length (g and d) and Accelerating elements, namely Cavities with a number of RF Cells, as shown in Figure 4. The summary of the RF and geometry parameters for the AGS Upgrade SCL is given in Table 1.

LONGITUDINAL EQUATIONS OF MOTION

Introduce the Time Delay $\tau = t - t_s$ and the Energy Difference $\varepsilon = E - E_s$. Let a prime denote derivative with respect to the path length. After linearization

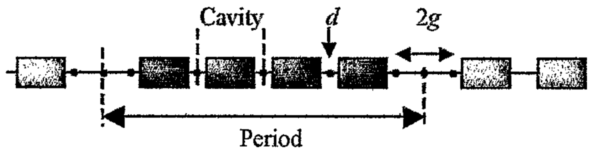

Figure 4. Arrangement of Periods, Cavities and Drifts

Table 1. AGS-Upgrade SCL

Linac Section	LE	ME	HE
Injection Energy, MeV	200	400	800
Final Energy, MeV	400	800	1,200
RF Frequency, MHz	805	1,610	1,610
Ave. Axial Field, MV/m	13.4	29.1	29.0
No. of Periods	6	9	8
No. of Cavities/Period, *M*	4	4	4
No. of Cells/Cavity, *N*	8	8	8
Cell Length, cm	11.45	7.03	7.92
Cavity Length, cm	91.60	56.24	63.36
Cavity Separation, *d*, cm	32	16	16
Warm-Cold Transition, cm	30	30	30
Warm Insertion, cm	107.9	137.9	137.9
Period Drift, *g*, cm	67.95	90.95	90.95

$$\tau' = -\varepsilon / c\, \beta_s^3\, \gamma_s^3\, E_0 \qquad (1)$$

$$\varepsilon' = -eE_{acc}\, (\sin \phi_s)\, \omega\tau \qquad (2)$$

where ϕ_s is the reference RF phase. For a segment of the accelerating structure, short enough to neglect the variation of $\beta_s^3\, \gamma_s^3$, by combining Eq.s (1) and (2)

$$\tau'' + K^2 \tau = 0 \qquad (3)$$

$$K = [eE_{acc}\, (-\sin \phi_s)\, \omega / c\, \beta_s^3\, \gamma_s^3\, E_0\,]^{1/2} \qquad (4)$$

MATRIX METHOD

The particle longitudinal motion can also be described with matrices (Ref. 2), in analogy to the method used to study transverse betatron oscillations. *Each transport matrix applies to a column vector of* components τ and τ'. The transfer matrix for a Drift of length ℓ is

$$M_{drift}(\ell) = \begin{vmatrix} 1 & 1 \\ 0 & 1 \end{vmatrix} \qquad (5)$$

and for a Cell of length L

$$M_{cavity} = \begin{vmatrix} \cos\theta & (\sin\theta)/K \\ -K\sin\theta & \cos\theta \end{vmatrix} \qquad (6)$$

Define $\theta = KL$ and $\eta = d / L$. When the various elements are multiplied together, we obtain the transfer matrix for a Cavity

$$M_c = M_{drift}(d/2)\, M_{cavity}\, M_{drift}(d/2) \qquad (7)$$

$$M_c = \begin{vmatrix} \cos\mu_c & \beta_c \sin\mu_c \\ -(\sin\mu_c)/\beta_c & \cos\mu_c \end{vmatrix} \qquad (8)$$

where

$$K\beta_c = (1 - \theta^2\eta^2/4 + \theta\,\eta\,\cot\theta\,)^{1/2} \qquad (9)$$

$$L\, tg\, \mu_c = \theta\, \beta_c / (\cot\theta - \theta\,\eta/2\,) \qquad (10)$$

Similarly the transfer matrix for a Period

$$M_p = M_{drift}(g)\, M_c^M\, M_{drift}(g) \qquad (11)$$

$$M_p = \begin{vmatrix} \cos\mu_p & \beta_p \sin\mu_p \\ -(\sin\mu_p)/\beta_p & \cos\mu_p \end{vmatrix} \qquad (12)$$

where

$$\beta_p = [\beta_c^2 - g^2 + 2\, g\, \beta_c \cot(M\mu_c)]^{1/2} \qquad (13)$$

$$L\, tg\, \mu_c = \beta_p / [\beta_c \cot(M\mu_c) - g] \qquad (14)$$

It is to be observed that the use of the transfer matrices M_c and M_p gives a good approximation when the energy gain across one Cavity section and, eventually, one Period is a small fraction of the energy in entrance.

Define the Bunch Area $S = \pi\, \Delta\tau\, \Delta\varepsilon$, the Bunch (Half) Length $\Delta\tau = (S_n\, \beta_{c,p} / \pi)^{1/2}$, and the normalized bunch area $S_n = S / c\, \beta_s^3\, \gamma_s^3\, E_0$.

STABILITY OF MOTION

The condition for stability is that | Trace of M_c and M_p | < 2, that is | $\cos\mu_{c,\,p}$ | is real and less than unit, and also $\beta_{c,\,p}$ is real and positive. The stability Diagrams are shown in Figures 5 and 6. It is seen that when the major drifts $d = g = 0$, the motion is always stable. Increasing the length of the drifts causes a reduction of the range of stability. Figure 7 gives the maximum value θ_{max} of the rotation angle, that is the accelerating gradient, versus the ratio η.

MISMATCH OF MOTION

We have assumed that K does not change across a *period*. This is justified if the acceleration rate is not too high, and the energy change is only a small fraction of the total kinetic energy. Exact matching is achieved by requiring that the amplitude value β_p remains constant from one period to the next. In turn that requires that also β_c and μ_c per cavity interval remain unchanged. That is the rotation angle θ and the restoring parameter K are also constant. For given RF angular frequency ω and phase ϕ_s, we derive the following condition for exact matching

$$E_{acc} / \beta_s^3 \gamma_s^3 = \text{constant} \tag{15}$$

A difficult condition to satisfy!

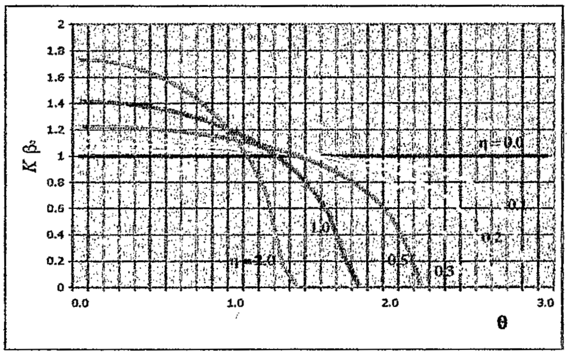

Figure 5. Plot of $K\beta_c$ versus θ for various values of η

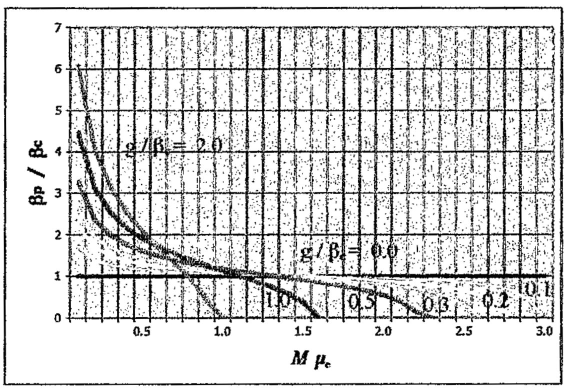

Figure 6. Plot of β_p / β_c vs. $M\mu_c$ for several values of g/β_c

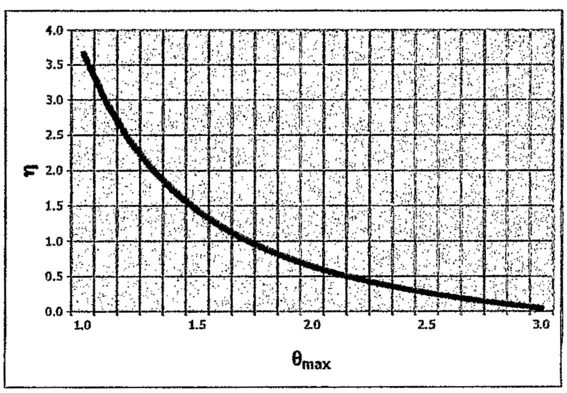

Figure 7. Plot of max value of θ versus η

A simpler mode of operation assumes a constant energy gain per *period*, so that the restoring parameter K will decrease with the beam energy. This will cause continuous mismatch of the particle motion, resulting in a beam bunch rotation (with *consequent possible dilution) of an amount that* depends on the acceleration rate, and on the length of the drift insertions (d and g). In analogy to the conventional approach used to describe the transverse betatron motion, a beam bunch can be made to correspond to an ellipse in the phase space (τ, τ'). Between periods, the ellipse is described by the amplitude β_p and the inclination α_p.

To estimate the amount of mismatch as the motion progress, we assume that the beam bunch is exactly matched at the entrance of the SCL section, where $\alpha_p = 0$. It is well know then how to estimate the bunch ellipse rotation, dilation or contraction from one period to the next with the transformation

$$\begin{vmatrix} \beta_p \\ \alpha_p \\ \gamma_p \end{vmatrix}_2 = \begin{vmatrix} m_{11}^2 & -2\, m_{11} m_{12} & m_{12}^2 \\ -m_{21}\, m_{11} & 1 + 2\, m_{12} m_{21} & -m_{12} m_{22} \\ m_{21} & -2\, m_{22}\, m_{21} & m_{22}^2 \end{vmatrix} \begin{vmatrix} \beta_p \\ \alpha_p \\ \gamma_p \end{vmatrix}_1 \tag{16}$$

$$\beta_p \gamma_p = 1 + \alpha_p^2 \tag{17}$$

Figure 8 shows some typical parameters in the Low-Energy section of the AGS-SCL that indicate how close is the stability limit (Ref. 3). The number of phase oscillations over one period is large when compared to that of circular accelerators. The inclination parameter α_p, a measure of the mismatch of motion, and the envelope amplitude function β_p are also shown, together to the bunch dimension.

Let then the equation of the longitudinal bunch ellipses

$$S_n/\pi = \gamma_p \tau^2 + 2\alpha_p \tau \tau' + \beta_p \tau'^2 \tag{18}$$

$$\tau' / \tau_0' = -\alpha\, \tau / \tau_0 + [1 - (\tau / \tau_0)^2]^{1/2} \tag{19}$$

where τ_0, τ_0' are the extensions in the (τ, τ') phase space. The evolution of the bunch ellipse is shown in Figure 9 at the end of each period for the AGS Low-Energy section in actual coordinates, whereas the same ellipses are also shown in Figure 10 using normalized coordinates (19). The continuous mismatch is noticeable.

CONCLUSIONS

Usually, our perception of a beam moving down an accelerator is made of bunches having the longitudinal shape of unchanging upright ellipses. This may be indeed a good approximation in circular accelerators where the energy gain per turn is small, but is not correct in the case of linear accelerators where the acceleration rate is considerably higher and

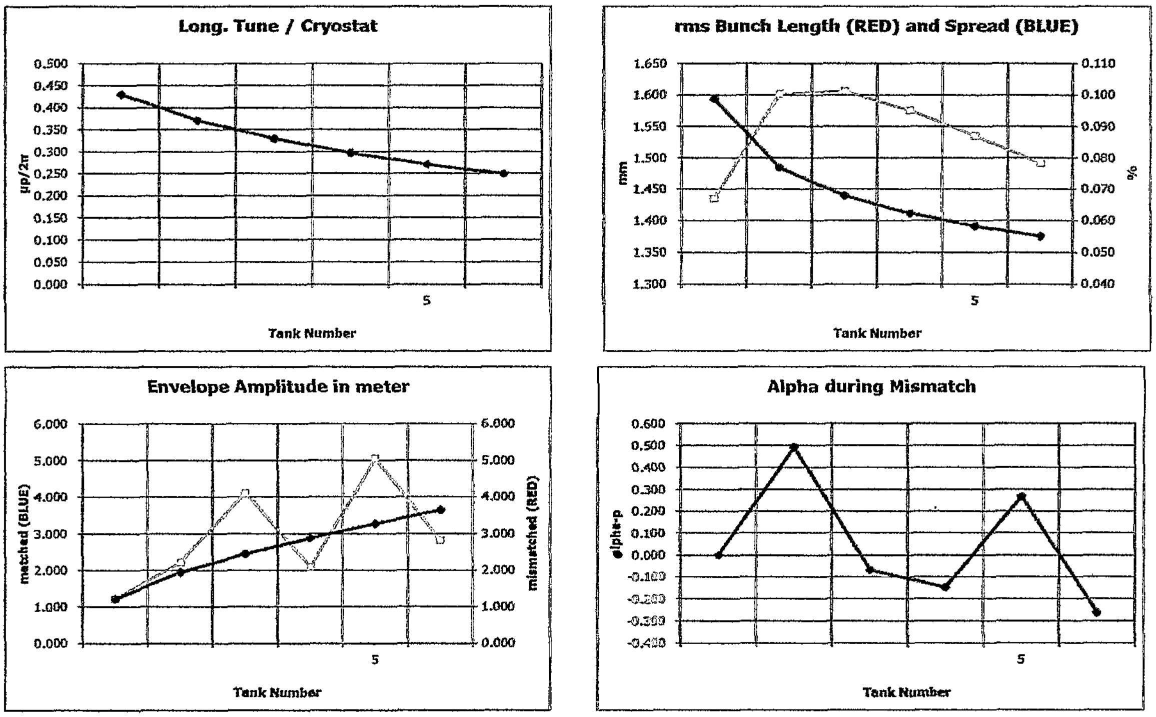

Figure 8. Variation of some bunch parameters with the period number.

the beam energy changes over short periods of length. Moreover, active accelerating cavities are separated by drifts of various lengths that introduce an intrinsic mismatch by which beam bunches actually rotate, elongate and contract over considerably short periods of length of only few meters. This has an analog with the transverse motion where also the betatron emittance ellipse changes continuously but periodically. The longitudinal motion nevertheless has no intrinsic periodicity and it is continuously mismatched from one location to the next. Our concern is that the continuous tumbling rapidly changing in a SCL of the bunches may lead to the creation of longitudinal halos accompanied by latent beam losses. Operation of high-power SCL in the GeV range needs to be demonstrated. There are several proton SCL projects being proposed, but only one is presently under construction (SNS) and will be soon, hopefully, in operation.

REFERENCES

1. A.G. Ruggiero et al., "AGS Upgrade to 1-MW with a Super-Conducting Linac Injector", presented at PAC03, Portland, Oregon, May 2003.
2. A.G. Ruggiero, "Design Considerations on a Proton Superconducting Linac", BNL-62312, Aug. 1995.
3. A Visual Basic Program for the Design of SCL, available by request to the Author.

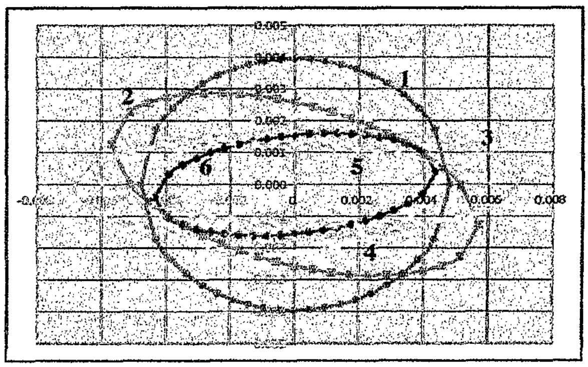

Figure 9. Bunch ellipses at the exit of each period of the SCL Low-Energy section.

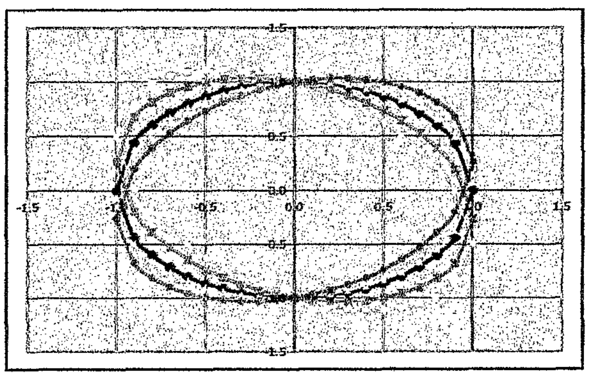

Figure 10. The same bunch ellipses in the variables τ'/τ_0' and τ/τ_0